Vol. 132: 13–22, 2018
https://doi.org/10.3354/dao03288

DISEASES OF AQUATIC ORGANISMS
Dis Aquat Org

Published December 11

Isolation and identification of pathogenic *Aeromonas veronii* from a dead Yangtze finless porpoise

Z. G. Liu[1,2,3], A. F. Zheng[2,3], M. M. Chen[2,3], Y. X. Lian[2,3], X. K. Zhang[2,3], S. Z. Zhang[2,3], D. Yu[2,3,*], J. K. Li[1,*,]**

[1]College of Veterinary Medicine, Huazhong Agricultural University, Wuhan 430070, PR China
[2]College of Life Science, Anqing Normal University, Anqing 246011, PR China
[3]Research Center of Aquatic Organism Conservation and Water Ecosystem Restoration in Anhui Province, Anqing Normal University, Anqing 246011, PR China

ABSTRACT: Diseases caused by *Aeromonas veronii* in freshwater fish have been widely reported, but other species such as aquatic mammals have probably been overlooked. Here, we identified one isolate of *A. veronii* from a Yangtze finless porpoise *Neophocaena asiaeorientalis asiaeorientalis* exhibiting disease and mortality, and subsequently confirmed its virulence in artificial infection of BALB/c mice. The bacterial isolate was identified as *A. veronii* based on physiological, biochemical, and phenotypic features, and homology of the 16S rRNA, *cpn60*, *rpoB*, *dnaJ* and *gyrB* genes. Our results expand the known host spectrum of *A. veronii*, which is of great importance for the etiology of porpoise, dolphin, and other cetacean diseases.

KEY WORDS: Yangtze finless porpoise · *Aeromonas veronii* · Isolation · Identification · Biological characteristics

1. INTRODUCTION

The Yangtze finless porpoise *Neophocaena asiaeorientalis asiaeorientalis* (YFP) is the only freshwater dolphin currently inhabiting the lower-middle reaches of the Yangtze River, and Dongting and Poyang lakes (Wang et al. 2008). With increases in human activities such as waterway regulation, port construction, sand dredging, water pollution, and illegal fishing, the habitat of the YFP has been severely damaged, resulting in a sharp decline in the population. At present, the population of the YFP is less than 1000 and is still decreasing at an annual rate of 13.7%, characterizing this as a Critically Endangered species (Mei et al. 2012, Wang et al. 2013).

Infectious diseases are now one of the most important factors that hinder the growth and breeding of the YFP, leading to a rapid decline in the population (Wan et al. 2016b, Wan et al. 2017). Data from the Ministry of Agriculture of the People's Republic of China show that 251 registered YFPs died between January 2008 and December 2016 (Liu et al. 2018). The causes of death of 97 of these YFPs were determined; 43% died from human activities and 25% from disease. Although some scholars have reported on the morbidity and mortality of the YFP, the cause of death is unknown in many cases (Zhao & Liu 2002, Guo et al. 2007). There are few studies on etiology, making disease prevention and management difficult for the YFP. *Pseudomonas aeruginosa* was isolated from a YFP that suffered from acute respiratory illness (Guo et al. 2007); *Aeromonas salmonicida* was found to cause skin diseases in YFP (Liu et al. 2017); and *Staphylococcus aureus* and *Morganella morganii* were identified as pathogenic bacteria in an infected YFP (Liu et al. 2018).

Aeromonas veronii is a type of conditional pathogen found widely in soil, water, and food. The bacterium infects many hosts, including *Ctenopharyngodon idelle*, *Perca fluviatilis*, *Cyprinus carpio*, *Oreochromis mossambicus*, *Megalobrama amblycephala*, *Anguilla japonica*, *Pelodiscus sinensis*, *Andrias davidianus*, *Vulpes* spp., and humans (Ormen et al. 2005, Janda & Abbott 2010, Silver et al. 2011, Pérez et al. 2015, Sun et al. 2016, Dong et al. 2017) in various ways, causing

*These authors contributed equally to this paper
**Corresponding author: lijk210@mail.hzau.edu.cn

septicemia, meningitis, diarrhea, and other symptoms (Rhee et al. 2016, Soltan Dallal et al. 2016, Chenia & Duma 2017). However, to date, there are no reports of YFPs being infected by *A. veronii*. In this study, we used microbiological and molecular biological methods to research and isolate, for the first time, pathogenic *A. veronii* from a dead YFP. The main pathological changes of the dead YFP were pleural effusion, pericardial effusion, hyperemia of multiple organs, hemorrhage, and degeneration. The results of this study expand the known host spectrum of *A. veronii*, which is of great importance for the etiology of porpoise, dolphin, and other cetacean diseases, and it provides essential scientific guidance for future health management of the YFP.

2. MATERIALS AND METHODS

2.1. Sample source

Samples were taken from a dead male YFP found in the Yangtze River. The YFP was found alive but was very weak, and died after rescue efforts failed.

2.2. Reagents

Trypticase soy agar (TSA), trypticase soy broth (TSB), ordinary nutrient agar, and Luria-Bertani culture medium were obtained from Qingdao Haibo Biotechnology. The bacterial genome extraction kit, PCR amplification related reagents, agarose, and DNA markers were obtained from Wuhan Guge Biotechnology. The 16S rRNA, *cpn60*, *rpoB*, *dnaJ and gyrB* primers were synthesized by Shanghai Bioengineering.

2.3. Necropsy and histopathological observation

Necropsy of the dead YFP was performed as described previously (Cozzi et al. 2016). Gross changes in each organ were observed and recorded. Organs (liver, lung, stomach, heart, kidneys, adrenal gland, heart coronary fat) with typical lesions were quickly separated from the body and stored in sterile containers with refrigeration; the samples were then quickly transferred to the laboratory and inoculated into culture medium after aseptic treatment. Organs with typical lesions were selected for microscopic histopathological observation. The samples were fixed in 4% paraformaldehyde for 24 h. After dehydration and embedding in paraffin, the paraffin blocks were cut into 4 µm tissue sections for hematoxylin and eosin (H&E) staining, examined by light microscopy, and photographed.

2.4. Bacterial isolation and identification

Organ samples with clear lesions (e.g. liver, lung, and lymph nodes) were aseptically inoculated onto TSA and cultured at 35°C for 24 h. Then, for purification, a single colony was inoculated onto TSA and cultured for 16–18 h at 35°C. Next, a single colony was selected for Gram staining and observed under a microscope. The shape, color, size, and other characteristics of the colony were recorded.

2.5. Determination of physicochemical properties

The purified strain (named JT-AV) was inoculated onto specific media for the identification of bacterial physicochemical properties, including the Voges-Proskauer (VP) test, the methyl red (MR) test, the oxidative-fermentative test, and so on, according to Bergey's Manual of Systematic Bacteriology and related identification manuals (Martin-Carnahan & Joseph 2005).

2.6. PCR amplification and gene sequence alignment

The bacterial genome extraction kit was used to extract genomic DNA which was used as a template in all PCR reactions. *Aeromonas veronii* was identified by 16S rRNA, *gyrB*, *rpoB*, *dnaJ*, and *cpn60* gene sequencing analysis. PCR primer design and amplification were based on published papers (Moreno et al. 2002, Soler et al. 2004, Küpfer et al. 2006, Nhung et al. 2007, Miñana-Galbis et al. 2009). The PCR products were tested by 0.8% agarose gel electrophoresis, and the positive samples were sequenced by Shanghai Bio-Engineering Technology. Reference gene sequences from pathogenic strains were obtained from the GenBank database of NCBI. Gene sequences were compared by BLAST.

2.7. Mouse pathogenicity test

After isolation, the frozen *A. veronii* JT-AV strain was inoculated into 1 ml TSB with a concentration of 2% and cultured at 35°C for 18 h. The bacterium was

collected after centrifuging at 3000 × *g* for 6 min, resuspended in 1 ml sterilized phosphate-buffered saline (PBS), and diluted 10- and 100-fold. The concentration of bacteria was measured in colony forming units (CFU) using the plate counting method. A total of 50 female lab mice (BALB/c; 4–5 wk old, specific pathogen free, 12–13 g) were randomly divided into 5 groups. Three groups were inoculated with 0.2 ml bacterial suspension, at concentrations of 3.46 × 10^7 CFU ml^{-1} (high dose; HD), 3.46 × 10^6 CFU ml^{-1} (moderate dose; MD), or 3.46 × 10^5 CFU ml^{-1} (low dose; LD), respectively. The fourth group was inoculated with PBS (PBS group), and the fifth group was not inoculated (blank) and served as a control. During the 10 d experiment, the mice were monitored daily, with body weight changes and death observed and recorded. Furthermore, gross pathological changes in each organ were observed and recorded at autopsy. The organs with typical lesions (liver, lung, brain, kidney) were selected for microscopic histopathological analysis, as described in 'Necropsy and histopathological observation', above.

This experiment was approved by the Animal Care and Ethics Committee of the Research Center of Aquatic Organism Conservation and Water Ecosystem Restoration in Anhui Province, China, considering national legislation regarding animal welfare. All mice had free access to feed and water.

3. RESULTS

3.1. Characteristics of the dead YFP

Physical and clinical examination indicated that the dead YFP was a male (body length 150 cm, weight 51 kg, max. circumference 88 cm, axillary girth 81 cm, ventral fat thickness 3.5 cm) in a well-nourished state. There was no obvious trauma to the skin. However, the bulbar conjunctiva was hemorrhaged. Anatomic examination revealed pericardial and pleural effusion, along with pulmonary hemorrhage and necrosis, myocardial hemorrhage, exudate of gelatinous sulcus coronarius fat, hepatic swelling, degeneration and necrosis, an empty stomach with hyperemia, and hemorrhage of the gastric mucosa (Fig. 1).

3.2. Histological analysis of the dead YFP

The pathological changes were as follows: severe pulmonary hemorrhage, accompanied by significant macrophage infiltration and pulmonary bronchiectasis congestion (Fig. 2A); focal hepatic necrosis, connective tissue hyperplasia, accompanied by fibrosis, sinusoidal dilatation, and inflammatory cell infiltration (Fig. 2B); gastric pit structure disappearance, mucosal focal necrosis accompanied by severe bleed-

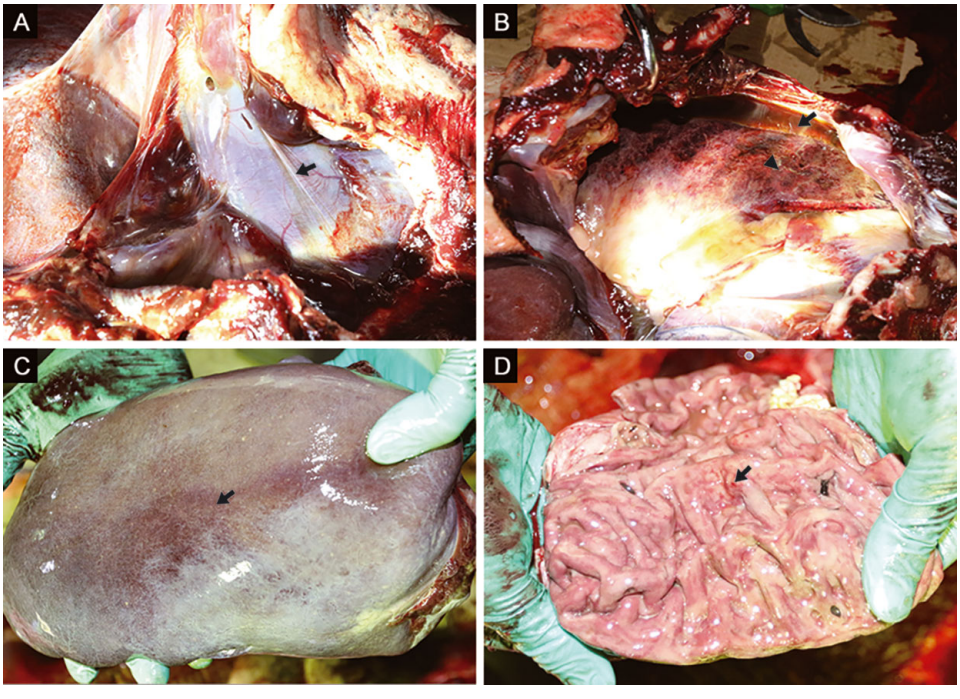

Fig. 1. Anatomical pathological changes observed in the dead Yangtze finless porpoise (YFP). (A) Pericardial effusion (arrow); (B) pleural effusion (arrow), pulmonary hemorrhage and necrosis (arrowhead); (C) hepatic degeneration and necrosis (arrow); (D) gastric hemorrhage and necrosis (arrow)

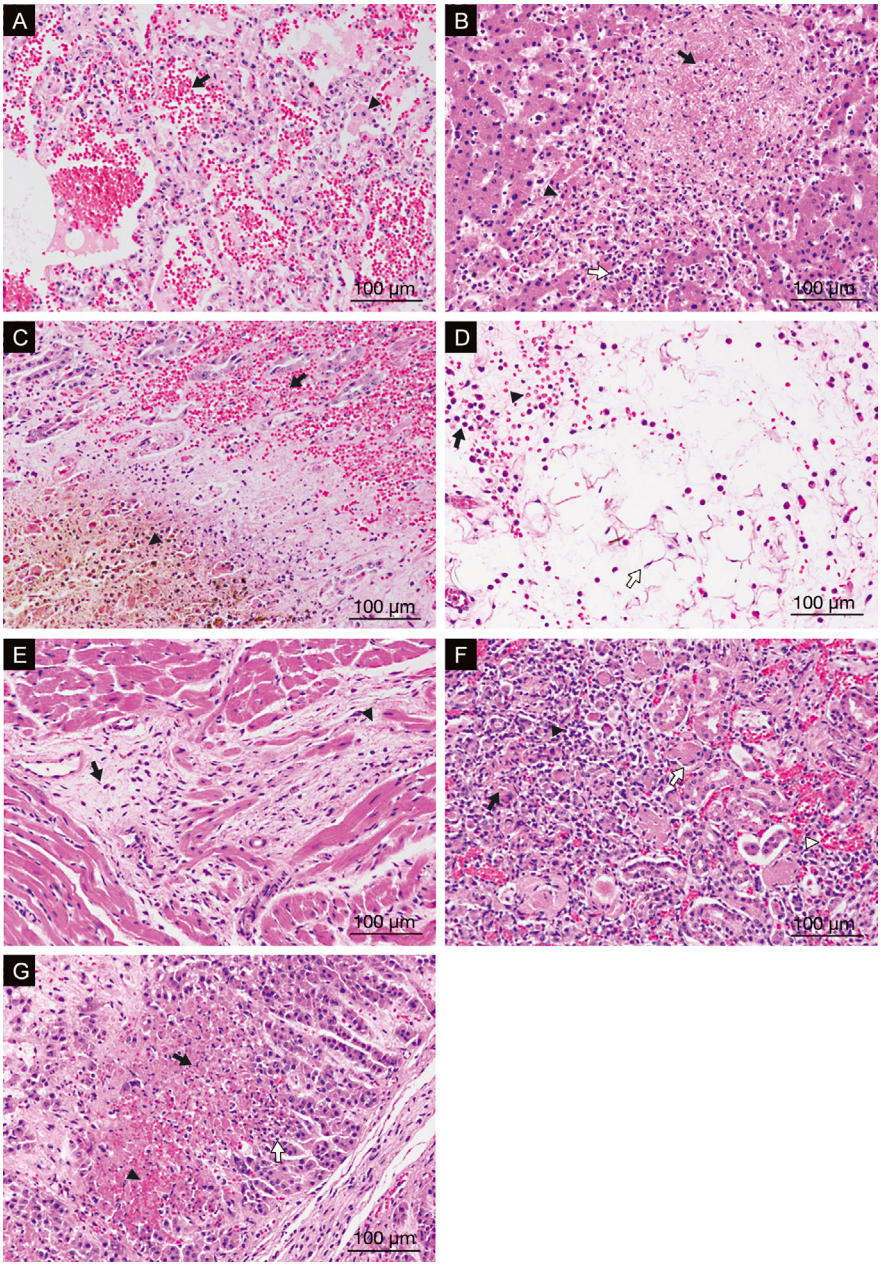

Fig. 2. Histopathological features of organs in the dead Yangtze finless porpoise (YFP) (hematoxylin and eosin [H&E] staining, 200×). (A) Lung tissue shows a large number of red blood cells and plasma in alveoli (black arrow), accompanied by a large number of macrophages (black arrowhead). (B) Liver tissue shows focal tissue necrosis with red stain, accompanied by connective tissue hyperplasia (black arrow), dead liver cells are seen around necrotic lesions, with nuclear condensation, enhanced cytoplasmic eosinophilia (black arrowhead), and a small amount of inflammatory cell infiltration (white arrow). (C) Gastric tissue shows gastric pit structure disappearance, gastric gland focal necrosis in the upper mucosal layer, accompanied by many hemosiderin depositions (black arrowhead), the number of gastric glands is reduced in the lower mucosal layer, accompanied by severe bleeding in the gland (black arrow). (D) Coronal fat tissue shows extensive necrosis of coronary adipocytes and rupture (black arrowhead), infiltration of inflammatory cells, mainly plasma cells (white arrow), and high free erythrocyte exudation (black arrow). (E) Heart tissue shows local loose connective tissue hyperplasia (black arrowhead) accompanied by a small amount of inflammatory cell infiltration (black arrow). (F) Renal tissue shows high local small blood vessel hyperplasia (black arrow), accompanied by inflammatory cell infiltration (black arrowhead) and some tubular necrosis: necrotic tubular epithelial cells are red stained, with or without a small nucleus (white arrow), there is renal interstitial capillary dilation and congestion (white arrowhead). (G) Adrenal gland shows local tissue necrosis with red-stained and nuclear fragments (black arrow), erythrocyte exudation in the necrotic area (black arrowhead), and a small amount of inflammatory cell infiltration at the edge of necrosis (white arrow)

ing (Fig. 2C); extensive necrosis of coronary adipocytes, rupture, infiltration of inflammatory cells, showing marked free erythrocyte exudation (Fig. 2D); local loose connective tissue hyperplasia in heart, accompanied by a small amount of inflammatory cell infiltration (Fig. 2E); notable small blood vessel hyperplasia in local renal tissue, accompanied by inflammatory cell infiltration (Fig. 2F); and local necrosis and bleeding in adrenal tissue (Fig. 2G).

3.3. Isolation and purification of bacteria

The bacteria grew to different degrees in Petri dishes after inoculation (Table 1). The characteristics of the isolate JT-AV were observed after purification. This isolate grew well on TSA medium. The colonies were round or oval in shape with a moist, smooth and opaque gray-white surface, with good growth at 35°C. Gram staining microscopy indicated that the isolates were Gram-negative, and 0.3–0.7 × 0.8–1.2 µm. The thallus was a short rod that was blunt at both round ends, no spores formed, and colonies often occurred singly (data not shown).

3.4. Determination of physicochemical properties

The results of bacterial physiological and biochemical identification indicate that the isolate used glucose and maltose. In contrast, the isolate could not use sucrose, lactose, gelatin, or sorbitol. The isolate was positive for urease, oxidase, phenylalanine, ornithine, and the MR test, but negative in the VP, DNA enzyme, and lysine tests (Table 2). The identifying features of the isolate were consistent with the biological description of *Aeromonas veronii* as suggested by Garrity et al. 2005). Therefore, the isolate was identified as *A. veronii*.

Table 1. Bacterial isolation and purification analysis in different organs of the dead Yangtze finless porpoise

Source	Isolated bacteria
Liver	*Aeromonas veronii*
Lung	*A. veronii*, *Micrococcus luteus*
Lymph nodes	*A. veronii*
Pericardial effusion	*A. veronii*
Pleural effusion	None
Kidney	*A. veronii*
Blowhole	*A. veronii*, *Acinetobacter junii*, *Bacillus licheniformis*, *Micrococcus luteus*

3.5. PCR amplification and gene sequence alignment

PCR products were detected and 500, 800, 900, 1100, and 1500 bp target fragments were observed (Fig. 3), which was consistent with the sequencing results. BLAST results revealed that the sequences were closely related to those from *A. veronii*, with 99% similarity (Table 3). Combining the bacterial morphological observations and physicochemical identification, the isolated bacteria was confirmed as *A. veronii*.

Table 2. Physicochemical identification and properties of the 3 JT-AV isolates obtained from the Yangtze finless porpoise. (+) positive; (–) negative; F: fermentation type

Test	Isolate JT-AV	Test	Isolate JT-AV
Gram stain	–	Voges-Proskauer	–
Gluconate	–	Methyl red	+
Glucose gas	+	Phenylalanine	+
Arabinose	–	Gelatin	–
Mannitol	–	Oxidase	+
Maltose	+	Sucrose	–
Hydrogen sulfide	–	Lactose	–
Lysine	–	DNase	–
Arginine	–	Sorbitol	–
Ornithine	+	Urease	+
Salicin	–	Oxidation-fermentation	F

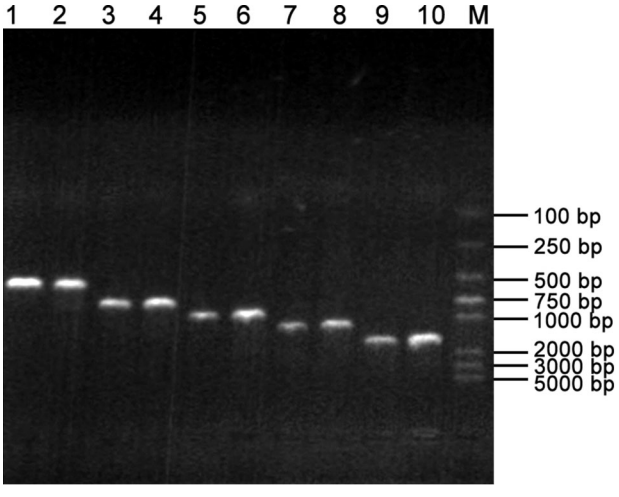

Fig. 3. Amplification of PCR products from the bacterial isolate JT-AV recovered from the dead Yangtze finless porpoise in this study. Lengths of the amplified fragments of *rpoB*, *cpn60*, *dnaJ*, *gyrB* and 16S rRNA were about 500, 800, 900, 1100, and 1500 bp respectively, which was consistent with the expected sizes of the target bands. Lanes: DNA marker (M), *rpoB* (1, 2), *cpn60* (3, 4), *dnaJ* (5, 6), *gyrB* (7, 8), and 16S rRNA (9, 10)

3.6. Mouse pathogenicity test

Pathogenicity test of strain *A. veronii* JT-AV in BALB/c mice showed that the isolated bacterium was strongly pathogenic. Mice in the 3.46 × 10^7 CFU ml^{-1} HD group died within 24 h of inoculation. The mortality of mice in the 3.46 × 10^6 CFU ml^{-1} MD group and the 3.46 × 10^5 CFU ml^{-1} LD group was 60 and 10% within 48 h of inoculation, respectively (Fig. 4A). In terms of body weight, there was a significant difference between the mice in the MD group and the other groups ($p < 0.05$). The body weight of mice in the MD group decreased clearly on the second day after infection, began to improve slowly on the fourth day after infection, and was fully recovered on the tenth day after infection. Although the body weight of mice in the LD group did not decline, the growth rate was slightly slower than that in the PBS and blank groups (not significant; Fig. 4B). Anatomical and histopathological observations of the dead mice indicated different degrees of effusion in the cavum thoracis and abdomen, intestinal tympanites, cerebral hyperemia, swelling, hepatic congestion and degeneration, pulmonary congestion, and hemorrhage (Fig. 5).

Histopathology findings were as follows: portal vein dilation, full of erythrocytes, resulting in congestion; liver cells around blood vessels showed fatty degeneration and varying sizes of round cavities in the cytoplasm (Fig. 6A). Pulmonary arteries, veins, and alveolar capillaries showed extensive dilatation, filled with red blood cells; local tissue bleeding, and large amounts of red blood cell aggregation in alveolar cavities (Fig. 6B). Capillary dilatation and congestion was present in brain tissue (Fig. 6C). There was also renal interstitial congestion, and protein casts in the tubular lumen filled with pink protein-like substances (Fig. 6D).

Table 3. Similarity between gene sequences from the isolated strain and published *Aeromonas veronii* sequences

Gene	GenBank ID	Similarity (%)
16S rRNA	MF401516	99
rpoB	MH590620	99
cpn60	MH590617	99
dnaJ	MH590618	99
gyrB	MH590619	99

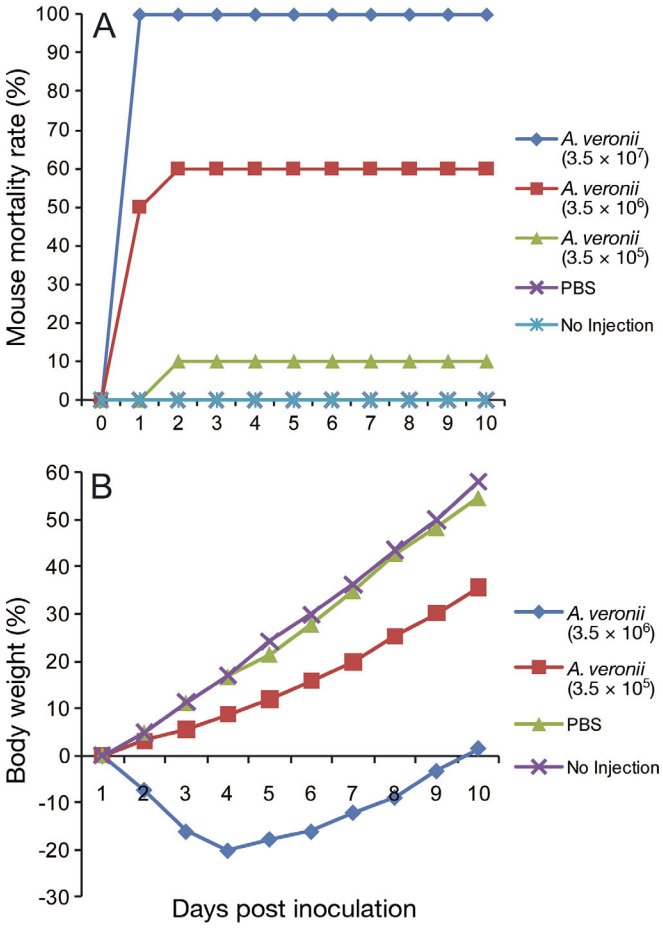

Fig. 4. (A) Daily cumulative percentage mortality and (B) growth of lab mice (BALB/c) after bacterial inoculation. Experimentally challenged BALB/c mice received 3.46 × 10^7, 3.46 × 10^6, or 3.46 × 10^5 colony forming units ml^{-1} of *Aeromonas veronii* by intraperitoneal injection. Control groups received either phosphate-buffered saline (PBS) medium or no injection. The infected mice were observed for 10 d

4. DISCUSSION

The YFP is a Critically Endangered species. Infectious disease is one of the main causes of its rapid population decline. To the best of our knowledge, this is the first report of the isolation and identification of pathogenic *Aeromonas veronii* from a dead YFP. *A. veronii*, a conditional pathogen and important zoonotic disease, is widely present in nature. It can infect many hosts, including fish (Ghatak et al. 2016, Adams et al. 2017, Dong et al. 2017, Hao et al. 2017, Jagoda et al. 2017), amphibians (Pearson et al. 2000), reptiles (Ye et al. 2012, Wimalasena et al. 2017), humans (Ottaviani et al. 2013, Chen et al. 2016, Soltan Dallal et al. 2016, Wang et al. 2016), and foxes (Li et al. 2012). To date, there are no reports of *A. veronii* in stranded or captive cetaceans (Bauer et al. 2016), and no reports of *A. veronii* infecting other marine mammals. In our study, we successfully iso-

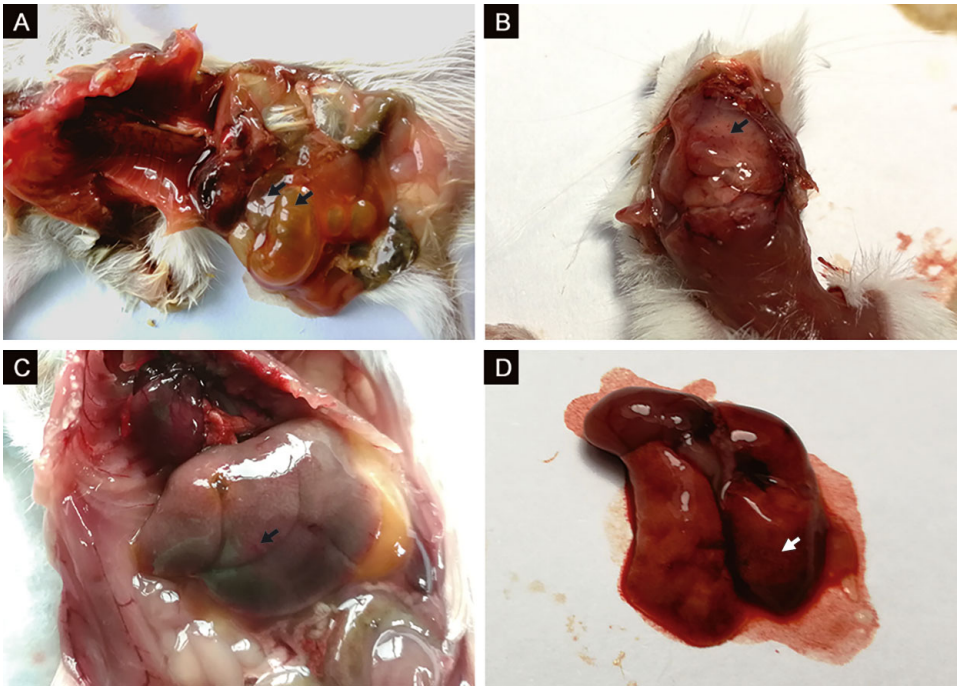

Fig. 5. Anatomic pathological changes observed in the dead lab mice after the pathogenicity test. (A) Effusion in cavum thoracis, abdomen, and intestinal tympanites (arrows); (B) cerebral hyperemia, swelling, and hemorrhage (arrow); (C) hepatic hyperemia and degeneration (arrow); (D) pulmonary hyperemia and hemorrhage (arrow)

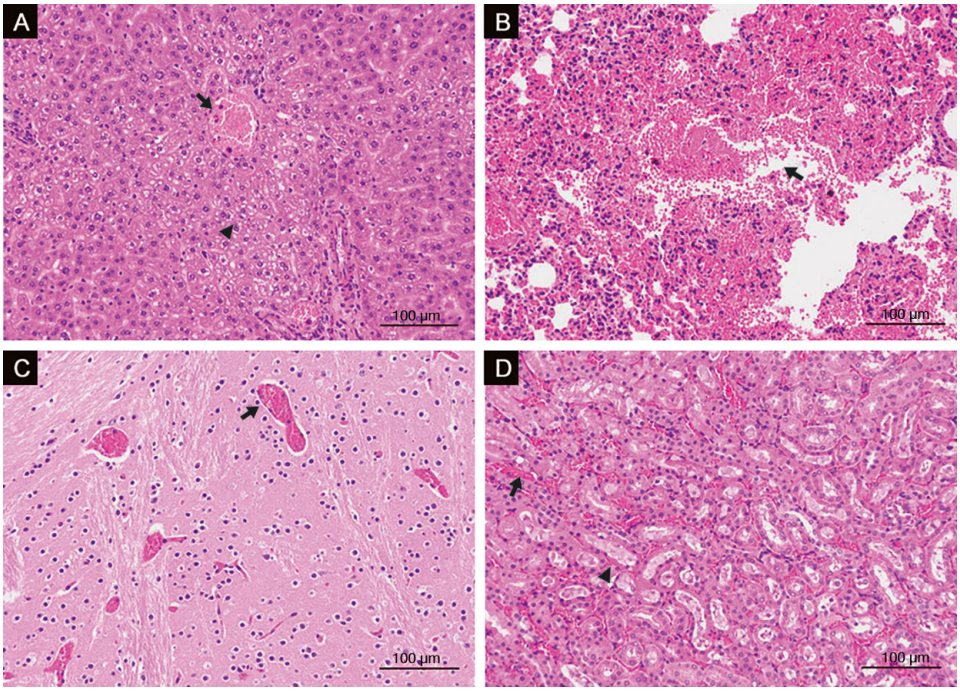

Fig. 6. Histopathological changes in lab mice infected with *Aeromonas veronii* (hematoxylin and eosin [H&E] staining, 200×). (A) Dilatation of the portal vein, full of red cells, presenting congestion (black arrow); and degeneration of hepatic fat cells with different sizes of circular vacuoles in the cytoplasm (black arrowhead); (B) hemorrhage in lung (black arrow); (C) capillary anapetia in brain tissue, full of red cells, and presenting congestion (black arrow); (D) protein casts are present in the tubular cavity filled with pink protein-like substances (black arrowhead); and renal interstitial vascular congestion (black arrow)

lated the pathogen and performed pathogenicity tests on it using BALB/c mice. Previous studies did not test the isolates for pathogenicity. The sampling sites in previous studies were also limited, mostly concentrated at sites such as blowholes (Zhao et al. 1998, Zhao & Liu 2002, Guo et al. 2007, Wan et al. 2016b). Although this sampling method has been used widely in the study of bacterial diversity of respiratory systems in cetaceans (Johnson et al. 2009, González-Hernández et al. 2010, Seabra de Lima et al. 2012), the isolation of pathogens by this method is limited and the sampling sites are susceptible to external environmental pollution. Here, we isolated the pathogen from multiple sites, in particular from organs with obvious lesions that had no contact with the external environment, and were therefore more likely to provide a pure pathogen culture.

Sequence comparison showed that the isolated JT-AV was highly homologous with many strains isolated from infected fish, such as *A. veronii* KF661548.1 and *A. veronii* FJ940848.1. The results indicate that *A. veronii* that infects fish and YFP may share the same origin. Studies have found that the *Aeromonas* that infects humans or animals is linked to the ingestion of contaminated food (Evangelista-Barreto et al. 2006, Chen et al. 2014). Because the food source of the YFP is mainly small fish, the YFP may have been infected by ingestion of infected fish. However, the disease transmission mechanism requires further study.

As the YFP is under national second-class protection, the pathogenicity of the isolated bacteria cannot be verified using the animal regression test. Therefore, we chose BALB/c mice for virulence verification. The *A. veronii* JT-AV strain had pathogenicity in the mouse model. The death and weight loss of mice varied with the dose. Previous studies have used BALB/c mice for the pathogenicity verification of *Brucella* isolated from marine mammals (Nymo et al. 2014, Larsen et al. 2016). These methods and reference indicators are in agreement with our experiment. Furthermore, in many cases, commensal pathogens that include *A. veronii* make the animal sick only when the immune function has declined or the body is stressed (Chopra et al. 2009, Avalos-Tellez et al. 2010, Zhang et al. 2016). Although we did not include such factors in our mouse infection experiments, the isolate still showed pathogenicity to mice. Whether such factors enhance the bacterial pathogenicity needs further study.

To date, much research has focused on marine mammal diseases, and numerous pathogens are known to be involved (Van Bressem et al. 2009, Jauniaux et al. 2010, Doss et al. 2017, Attademo et al. 2018). The epidemiology of some animal diseases has been extensively investigated (Hernández-Mora et al. 2017, Whatmore et al. 2017). Because of issues such as the difficulty involved with obtaining sample material and the lack of research, disease-related studies on the YFP are rare. There has been limited research on pathogens, mainly concentrating on bacterial and parasitic diseases (Wan et al. 2016a, Liu et al. 2017) while others, such as viral diseases, have not been addressed. Furthermore, the prevalence of disease in the YFP at different growth stages or during different seasons has not been systematically investigated. Therefore, further epidemiological studies are required on YFP to better understand the scientific basis of how disease affects the YFP and leads to mortality. In addition, preventive measures should be taken to control the spread of infections in this endangered species.

The successful isolation and identification of *A. veronii* in the YFP expands the host spectrum of *A. veronii*. It also provides a basis for the establishment of a diagnostic method for YFP disease, and for investigating the invasion and transmission mechanisms of related important pathogens and screening of therapeutic drugs.

Acknowledgements. We sincerely thank Zhang Suzi and Jiang Huyan (College of Life Science, Anqing Normal University, China) for their assistance with sample collection and mice pathogenicity testing. This work was supported by the Anhui University Provincial Natural Science Research Project (grant number KJ2017A357) and the Open Fund for the State Key Laboratory of Tropical and Subtropical Fishery Resource Application and Cultivation Microbiology (grant number KF20170101).

LITERATURE CITED

Adams RJ, Mathys DA, Mollenkopf DF, Whittle A, Daniels JB, Wittum TE (2017) Carbapenemase-producing *Aeromonas veronii* disseminated in the environment of an equine specialty hospital. Vector Borne Zoonotic Dis 17: 439–442

Attademo FLN, Silva JCR, Luna FO, Ikeda J and others (2018) Retrospective survey for pathogens in stranded marine mammals in northeastern Brazil: *Brucella* spp. infection in a Clymene dolphin (*Stenella clymene*). J Wildl Dis 54:151–155

Avalos-Tellez R, Suarez-Guemes F, Carrillo-Casas EM, Hernandez-Castro R (2010) Bacteria and yeast normal microbiota from respiratory tract and genital area of bottlenose dolphins (*Tursiops truncatus*). In: Mendez-Vilas A (ed) Current research, technology and education topics in applied microbiology and microbial biotechnology, Vol 1. Formatex Research Center, Malaga, p 666–673

Bauer KL, Goertz CE, Belovarac JA, Walton RW, Dunn JL, Tuomi P (2016) Infectious disease and toxicological monitoring of stranded pacific harbor seals (*Phoca vitulina richardsi*) in Cook Inlet as surrogates for monitoring endangered belugas (*Delphinapterus leucas*). J Zoo Wildl Med 47:770–780

Chen PL, Wu CJ, Tsai PJ, Tang HJ and others (2014) Virulence diversity among bacteremic *Aeromonas isolates*: *ex vivo*, animal, and clinical evidences. PLOS ONE 9: e111213

Chen PL, Lamy B, Ko WC (2016) *Aeromonas dhakensis*, an increasingly recognized human pathogen. Front Microbiol 7:793

Chenia HY, Duma S (2017) Characterization of virulence, cell surface characteristics and biofilm-forming ability of *Aeromonas* spp. isolates from fish and sea water. J Fish Dis 40:339–350

Chopra AK, Graf J, Horneman AJ, Johnson JA (2009) Virulence factor-activity relationships (VFAR) with specific emphasis on *Aeromonas* species (spp.). J Water Health 07(Suppl 1):S29–S54

Cozzi B, Huggenberger S, Oelschläger HA (2016) Anatomy of dolphins: insights into body structure and function. Academic Press, Amsterdam

Dong HT, Techatanakitarnan C, Jindakittikul P, Thaiprayoon A and others (2017) *Aeromonas jandaei* and *Aeromonas veronii* caused disease and mortality in Nile tilapia, *Oreochromis niloticus* (L.). J Fish Dis 40:1395–1403

Doss J, Culbertson K, Hahn D, Camacho J, Barekzi N (2017) A review of phage therapy against bacterial pathogens of aquatic and terrestrial organisms. Viruses 9:50

Evangelista-Barreto NS, Vieira RH, Carvalho FC, Torres RC, Sant'Anna ES, Rodrigues DP, Reis CM (2006) *Aeromonas* spp. isolated from oysters (*Crassostrea rhizophorea*) from a natural oyster bed, Ceara, Brazil. Rev Inst Med Trop São Paulo 48:129–133

Garrity G, Brenner DJ, Krieg NR, Staley JR (2005) The *Gammaproteobacteria*, Order XII, *Aeromonadales* ord. nov. In: Martin-Carnahan A (ed) Bergey's manual of systematic bacteriology, Vol 2, Part B: The *Proteobacteria*. Springer, Berlin, p 556–587

Ghatak S, Blom J, Das S, Sanjukta R and others (2016) Pangenome analysis of *Aeromonas hydrophila*, *Aeromonas veronii* and *Aeromonas caviae* indicates phylogenomic diversity and greater pathogenic potential for *Aeromonas hydrophila*. Antonie Leeuwenhoek 109:945–956

González-Hernández M, Denoel M, Duffus AJ, Garner TW, Cunningham AA, Acevedo-Whitehouse K (2010) Dermocystid infection and associated skin lesions in free-living palmate newts (*Lissotriton helveticus*) from southern France. Parasitol Int 59:344–350

Guo Z, Zhao QZ, Zhang XF (2007) Diagnosis and treatment of pneumonia caused by *Pseudomonas aeruginosa* in a Yangtze finless porpoise (*Neophocaena phocaenoides asiaeorientalis*). Shou Lei Xue Bao 27:86–91

Hao K, Wu ZQ, Li DL, Yu XB, Wang GX, Ling F (2017) Effects of dietary administration of *Shewanella xiamenensis* A-1, *Aeromonas veronii* A-7, and *Bacillus subtilis*, single or combined, on the grass carp (*Ctenopharyngodon idella*) intestinal microbiota. Probiotics Antimicrob Proteins 9:386–396

Hernández-Mora G, Bonilla-Montoya R, Barrantes-Granados O, Esquivel-Suárez A and others (2017) Brucellosis in mammals of Costa Rica: an epidemiological survey. PLOS ONE 12:e0182644

Jagoda SSSDS, Honein K, Arulkanthan A, Ushio H, Asakawa S (2017) Genome sequencing and annotation of *Aeromonas veronii* strain Ae52, a multidrug-resistant isolate from septicaemic gold fish (*Carassius auratus*) in Sri Lanka. Genom Data 11:46–48

Janda JM, Abbott SL (2010) The genus *Aeromonas*: taxonomy, pathogenicity, and infection. Clin Microbiol Rev 23: 35–73

Jauniaux TP, Brenez C, Fretin D, Godfroid J and others (2010) *Brucella ceti* infection in harbor porpoise (*Phocoena phocoena*). Emerg Infect Dis 16:1966–1968

Johnson SP, Venn-Watson SK, Cassle SE, Smith CR, Jensen ED, Ridgway SH (2009) Use of phlebotomy treatment in Atlantic bottlenose dolphins with iron overload. J Am Vet Med Assoc 235:194–200

Küpfer M, Kuhnert P, Korczak BM, Peduzzi R, Demarta A (2006) Genetic relationships of *Aeromonas* strains inferred from 16S rRNA, *gyrB* and *rpoB* gene sequences. Int J Syst Evol Microbiol 56:2743–2751

Larsen AK, Godfroid J, Nymo IH (2016) *Brucella pinnipedialis* in hooded seal (*Cystophora cristata*) primary epithelial cells. Acta Vet Scand 58:9

Li WJ, Zhao Y, Liu Y, Qi XX, Kang K, Chen M (2012) Isolation and identification of pathogenic *Aeromonas veronii* from fox. Chin J Prev Vet Med 34:289–292

Liu ZG, Jiang HY, Zhang XK, Chen MM, Wan A, Yu DP (2017) Identification and characterizations of *Aeromonas salmonicida* isolated from Yangtze finless porpoise. Shou Lei Xue Bao 37:1–11

Liu ZG, Zheng AF, Chen MM, Lian YX, Jiang HY, Yu DP (2018) Diagnosis and treatment of the bacterial diseases in the Yangtze finless porpoise. Acta Hydrobiologica Sinica 42:584–592

Martin-Carnahan AM, Joseph SW (2005) Genus I. *Aeromonas* Stanier 1943, 213[AL]. In: Brenner DJ, Krieg NR, Staley JT, Garrity GM (eds) Bergey's manual of systematic bacteriology. Springer, New York, NY, p 557–578

Mei Z, Huang SL, Hao Y, Turvey ST, Gong W, Wang D (2012) Accelerating population decline of Yangtze finless porpoise (*Neophocaena asiaeorientalis asiaeorientalis*). Biol Conserv 153:192–200

Miñana-Galbis D, Urbizu-Serrano A, Farfán M, Fusté MC, Lorén JG (2009) Phylogenetic analysis and identification of *Aeromonas* species based on sequencing of the *cpn60* universal target. Int J Syst Evol Microbiol 59: 1976–1983

Moreno C, Romero J, Espejo RT (2002) Polymorphism in repeated 16S rRNA genes is a common property of type strains and environmental isolates of the genus *Vibrio*. Microbiology 148:1233–1239

Nhung PH, Hata H, Ohkusu K, Noda M, Shah MM, Goto K, Ezaki T (2007) Use of the novel phylogenetic marker *dnaJ* and DNA–DNA hybridization to clarify interrelationships within the genus *Aeromonas*. Int J Syst Evol Microbiol 57:1232–1237

Nymo IH, das Neves CG, Tryland M, Bardsen BJ and others (2014) *Brucella pinnipedialis* hooded seal (*Cystophora cristata*) strain in the mouse model with concurrent exposure to PCB 153. Comp Immunol Microbiol Infect Dis 37: 195–204

Ormen O, Granum PE, Lassen J, Figueras MJ (2005) Lack of agreement between biochemical and genetic identification of *Aeromonas* spp. APMIS 113:203–207

Ottaviani D, Leoni F, Rocchegiani E, Santarelli S and others (2013) A severe case of *Aeromonas veronii* biovar sobria

travellers' diarrhoea characterized by *Vibrio parahaemolyticus* co-isolation. J Med Microbiol 62:161–164

Pearson MD, Hirono I, Aoki T, Miranda R, Inglis V (2000) Virulence properties of motile aeromonads isolated from farmed frogs *Rana tigerina* and *R. rugulosa*. Dis Aquat Org 40:185–193

Pérez L, Abarca ML, Latif-Eugenín F, Beaz-Hidalgo R, Figueras MJ, Domingo M (2015) *Aeromonas dhakensis* pneumonia and sepsis in a neonate Risso's dolphin *Grampus griseus* from the Mediterranean Sea. Dis Aquat Org 116:69–74

Rhee JY, Jung DS, Peck KR (2016) Clinical and therapeutic implications of *Aeromonas* bacteremia: 14 years nationwide experiences in Korea. Infect Chemother 48:274–284

Seabra de Lima IM, de Andrade LG, Ramos de Carvalho R, Lailson-Brito J, de Freitas Azevedo A (2012) Characteristics of whistles from rough-toothed dolphins (*Steno bredanensis*) in Rio de Janeiro coast, southeastern Brazil. J Acoust Soc Am 131:4173–4181

Silver AC, Williams D, Faucher J, Horneman AJ, Gogarten JP, Graf J (2011) Complex evolutionary history of the *Aeromonas veronii* group revealed by host interaction and DNA sequence data. PLOS ONE 6:e16751

Soler L, Yáñez MA, Chacon MR, Aguilera-Arreola MG, Catalán V, Figueras MJ, Martínez-Murcia AJ (2004) Phylogenetic analysis of the genus *Aeromonas* based on two housekeeping genes. Int J Syst Evol Microbiol 54: 1511–1519

Soltan Dallal MM, Mazaheri Nezhad Fard R, Kavan Talkhabi M, Aghaiyan L, Salehipour Z (2016) Prevalence, virulence and antimicrobial resistance patterns of *Aeromonas* spp. isolated from children with diarrhea. Germs 6:91–96

Sun J, Zhang X, Gao X, Jiang Q, Wen Y, Lin L (2016) Characterization of virulence properties of *Aeromonas veronii* isolated from diseased Gibel carp (*Carassius gibelio*). Int J Mol Sci 17:496

Van Bressem MF, Raga JA, Di Guardo G, Jepson PD and others (2009) Emerging infectious diseases in cetaceans worldwide and the possible role of environmental stressors. Dis Aquat Org 86:143–157

Wan X, McLaughlin RW, Zhou J, Hao Y, Zheng J, Wang D (2016a) Isolation of culturable aerobic bacteria and evidence of *Kerstersia gyiorum* from the blowhole of captive Yangtze finless porpoises. Antonie Leeuwenhoek 109: 1167–1175

Wan X, Ruan R, McLaughlin RW, Hao Y, Zheng J, Wang D (2016b) Fecal bacterial composition of the endangered Yangtze finless porpoises living under captive and semi-natural conditions. Curr Microbiol 72:306–314

Wan XL, Zheng JS, Li WX, Zeng XY, Yang JW, Hao YJ, Wang D (2017) Parasitic infections in the East Asian finless porpoise *Neophocaena asiaeorientalis sunameri* living off the Chinese Yellow/Bohai Sea coast. Dis Aquat Org 125:63–71

Wang JY, Frasier TR, Yang SC, White BN (2008) Detecting recent speciation events: the case of the finless porpoise (genus *Neophocaena*). Heredity 101:145–155

Wang D, Turvey ST, Zhao X, Mei Z (2013) *Neophocaena asiaeorientalis* ssp. *asiaeorientalis*. The IUCN Red List of threatened species 2013:e.T43205774A45893487

Wang W, Wang D, Zhu L, Fu Y and others (2016) Infection status and virulent genes of *Aeromonas* in diarrhea patients in Pudong New Area, Shanghai. Zhonghua Liu Xing Bing Xue Za Zhi 37:402–405 (in Chinese)

Whatmore AM, Dawson C, Muchowski J, Perrett LL and others (2017) Characterisation of North American *Brucella* isolates from marine mammals. PLOS ONE 12: e0184758

Wimalasena SHMP, De Silva BCJ, Hossain S, Pathirana HNKS, Heo GJ (2017) Prevalence and characterisation of quinolone resistance genes in *Aeromonas* spp. isolated from pet turtles in South Korea. J Glob Antimicrob Resist 11:34–38

Ye Y, Jiang Y, Fan T, Jiang Q, Cheng Y, Lu J, Lin L (2012) Resistance characterization, virulence factors, and ERIC-PCR fingerprinting of *Aeromonas veronii* strains isolated from diseased *Trionyx sinensis*. Foodborne Pathog Dis 9: 1053–1055

Zhang N, Jovanovic G, McDonald C, Ces O, Zhang X, Buck M (2016) Transcription regulation and membrane stress management in enterobacterial pathogens. Adv Exp Med Biol 915:207–230

Zhao QZ, Liu RJ (2002) The diagnosis and treatment for the common diseases of the alimentary canal in *Lipontes vexillifer* and *Neophocaena phocaenoides asiaeorientalis*. Shou Lei Xue Bao 22:237–240

Zhao QZ, Gong WM, Liu RJ (1998) Clinical observation and pathological diagnosis of the two cases of porpoise disease. Zhongguo Xumu Zazhi 16:381–389

Editorial responsibility: Andrew Barnes, Brisbane, Queensland, Australia

Submitted: February 7, 2018; Accepted: August 28, 2018
Proofs received from author(s): November 20, 2018